http://dx.doi.org/10.5012/bkcs.2014.35.3.958

Synthesis and Surface-Enhanced Raman Scattering Property of Pentagonal Dodecahedral Au Nanocrystals†

Minjung Kim, Gyoung Hwa Jeong,[a] Young Wook Lee, and Sang Woo Han*

Department of Chemistry and KI for the NanoCentury, KAIST, Daejeon 305-701, Korea. E-mail: sangwoohan@kaist.ac.kr
Received September 30, 2013, Accepted October 3, 2013

Key Words : Au, Nanocrystals, Pentagonal dodecahedron, SERS

The controlled synthesis of polyhedral Au nanocrystals (NCs) has attracted tremendous research interest in the past decades due to their promising applications in a variety of fields, such as plasmonics, sensors, electronics, catalysis, and surface-enhanced Raman scattering (SERS).[1-11] Since the inherent plasmonic, electrical, and catalytic properties of Au NCs can be finely tuned by control over their shapes, numerous synthesis methods have been developed for the production polyhedral Au NCs with tailored morphologies, such as Platonic solids (tetrahedron,[1] cube,[2] octahedron,[3] and icosahedron[4]), cuboctahedron,[5] decahedron,[6] rod,[7] and plate.[8] To minimize the surface energy during the NC growth, these Au NCs are mostly enclosed by stable low-index {111} and/or {100} facets. Recently, the synthesis of Au NCs with exposed high-energy facets, *i.e.*, low-index {110} and high-index {*hkl*} (at least one index greater than 1), has been reported.[9-11] NCs bound by high-energy facets have shown enhanced performance compared to conventional {111} and/or {100}-faceted NCs due to the presence of high-density undercoordinated atoms on their surfaces as well as to their unique morphological characteristics. For instance, we reported that rhombic dodecahedral (RD)[9] and hexoctahedral Au NCs[11] exclusively bound by {110} and {321} facets, respectively, exhibited pronounced SERS activities. Nevertheless, it is still a great challenge to synthesize shape-controlled NCs that are enclosed by high-index facets due to their high surface energy.

Here we report for the first time on the synthesis of pentagonal dodecahedral (PD) Au NCs bound by high-index {*hk0*} facets. The PD Au NCs could be readily prepared by the reduction of Au precursors with *N*,*N*-dimethylformamide (DMF) in the presence of poly(vinyl pyrrolidone) (PVP). The pentagonal dodecahedron is a convex polyhedron with 12 pentagonal faces, where 3 faces meet at each corner. The surface facets of PD structures have been determined to be high-index {*hk0*}: the simplest one is {210} and other types are {320}, {410}, and {120}.[12] The pentagonal dodecahedron has been known as a very unusual structure and crystalline materials with this structure have been rarely reported. Only the crystal of pyrite and some quasi crystals have this structure.[13] To the best of our knowledge, the synthesis of metal NCs with PD structure has never been reported. Furthermore, the prepared PD Au NCs could be successfully applied in the field of SERS. Highly enhanced SERS signals could be obtained from various analytes with the PD Au NCs, which can be attributed to their high-surface energy facets.

Figure 1(a) and (b) show representative low- and high-magnification field-emission scanning electron microscopy (FESEM) images of the as-prepared samples, demonstrating the formation of Au NCs with a well-defined structure. The sizes of Au NCs were in the range of 150-200 nm. The SEM image of NCs, shown in Figure 1(b), is closely matched by the 3D models of dodecahedra with different orientations (Figure 1(c)), indicating the successful generation of PD Au NCs enclosed by 12 pentagons under our experimental conditions. The X-ray diffraction (XRD) pattern of the PD Au NCs showed distinct diffraction peaks from the face centered cubic (*fcc*) structure of Au, revealing their crystalline nature (Figure 1(d)).

Figure 2(a) shows the transmission electron microscopy (TEM) image of a PD Au NC recorded along the [110] direction. The corresponding convergent beam electron diffraction (CBED) pattern is also shown in Figure 2(b), which

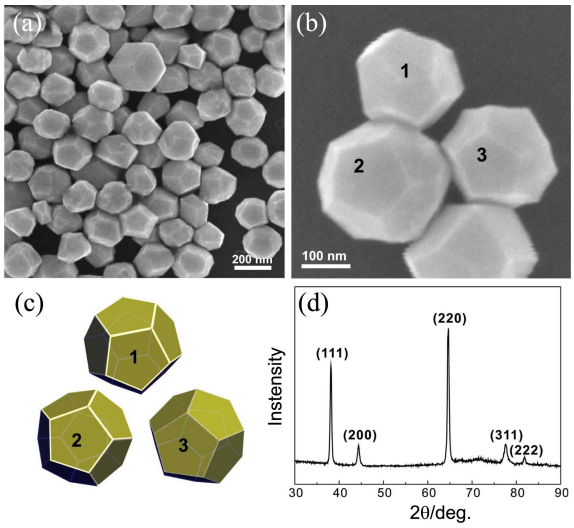

Figure 1. (a) Low- and (b) high-magnification FESEM images of the PD Au NCs. (c) 3D models of ideal dodecahedra in different orientations corresponding to the NCs marked with the identical number in (b). (d) XRD pattern of the PD Au NCs.

†This paper is to commemorate Professor Myung Soo Kim's honourable retirement.

[a]Present address: Center of Molecular Science and Technology, Ajou University, Suwon 443-749, Korea

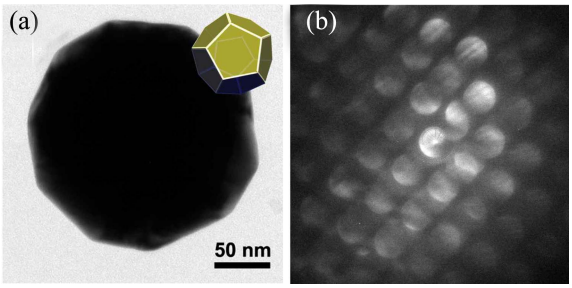

Figure 2. (a) TEM image and (b) corresponding CBED pattern of a PD Au NC recorded along the [110] direction. Model of ideal dodecahedron with the identical orientation is shown in the inset of (a).

confirms the orientation of the NC. The decagonal structure of the NC in the TEM image matched well the 2D projection of a corresponding geometric model of dodecahedron with the identical orientation (inset of Figure 2(a)). We cannot obtain the clear high-resolution surface image of the PD Au NCs due to their large thickness. Thereby, the surface facet of the PD Au NCs cannot be exactly identified at the present. However, we can assume that the PD Au NCs are enclosed by high-index {210} facets by consulting the PD structures reported in the literature.[12]

In a previous work, we report that the RD Au NCs enclosed by 12 {110} facets can be synthesized in high-yield by using DMF as both a reductant and a solvent without any seeds, surfactants, or foreign metal ions.[9] The kinetically-controlled growth of NCs at relatively low-temperature and the stabilization of unstable {110} facets by DMF or one of its oxidation products should contribute to the formation of the RD Au NCs. In the present work, the production of the PD Au NCs was achieved by the reduction of Au precursors with DMF in the presence of PVP under otherwise similar synthesis conditions with that used in the preparation of the RD Au NCs. This indicates that PVP plays a crucial role in the formation of the PD Au NCs. The crystal growth rates along different directions are proportional to their surface energies. For Au with *fcc* structure, the surface energy (γ) of different crystallographic planes follows the order $\gamma_{\{hkl\}} > \gamma_{\{110\}} > \gamma_{\{100\}} > \gamma_{\{111\}}$.[14] However, the precise values of the respective surface energies can be drastically influenced by the adsorption of chemical species, such as ions and surfactants. For instance, it has been known that PVP can stabilize the low-surface energy facets of *fcc* metal NCs through the adsorption of its polymer units on the growing NCs, thus can have control over the final NC morphology.[15] On the basis of this fact, we can propose that the generation of the PD Au NCs bound by high-index {210} facets under our experimental conditions can be facilitated *via* the stabilization of both {110} and {100} facets, respectively, by DMF and PVP during the NC growth.

Further control experiments confirmed this proposition. In the standard synthesis of the PD Au NCs, the molar ratio between the Au precursor and the monomer of PVP (vinyl pyrrolidone) was set to 1:45, because it has been proved an optimal value for the production of well-defined PD Au

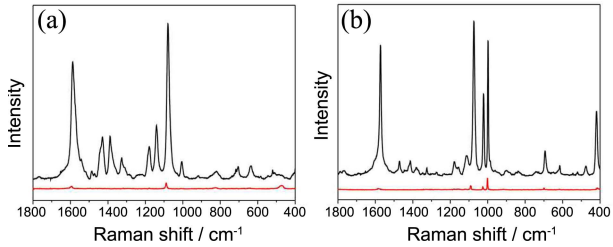

Figure 3. SERS spectra of (a) 4-ABT and (b) BT obtained with the PD Au NCs (upper trace). Normal Raman spectra of 4-ABT and BT are shown in the lower traces.

NCs. Lower or higher concentration of PVP than that used in the standard condition led to the formation of various-shaped NCs with low-index facets (data not shown). On the other hand, shorter or longer chain length of PVP than that employed in the standard synthesis (M_w = 630,000) did not yield the PD Au NCs (data not shown). These findings unequivocally reveal that fine control over the relative growth rate between {110} and {100} facets of growing NCs by employing an appropriate amount of PVP with a suitable chain length are indispensable for the successful formation of the PD Au NCs.

We expect that the exposed high-index surfaces of the prepared NCs can benefit various applications, especially in the field of SERS, because such high-energy surfaces have higher SERS activity than low-energy ones. To investigate the SERS efficiency of the PD Au NCs, we measured SERS spectra of 4-aminobenzenthoil (4-ABT) and benzenethiol (BT) adsorbed on the PD Au NCs. As shown in Figure 3, the PD Au NCs gave efficient SERS signals from the analyte molecules. Through the comparison with normal Raman spectra of analytes, Raman scattering enhancement factors (EF) of the PD Au NCs were calculated to be 1.76×10^5 and 4.50×10^4 for 4-ABT and BT, respectively, which are higher than those for conventional low-index-faceted spherical Au nanoparticles[16] despite their large particle sizes.

In summary, we have presented for the first time the synthesis method for the generation of PD Au NCs bound by 12 high-index facets. Precise tuning of the NC growth habit by adjusting the chain length as well as the relative amount of PVP is the key to the formation of this unprecedented structure. The prepared NCs exhibited efficient SERS properties due to their exposed high-energy facets. Since the synthesized NCs have unique structural and optical properties, they can be used as functional materials in a number of optical and catalytic applications.

Experimental

In a typical synthesis of PD Au NCs, an aqueous solution (10 mM, 1 mL) of $HAuCl_4 \cdot 3H_2O$ (99.9+%, Aldrich) was added to 25 mL of DMF. This solution was heated at 90 °C for about 2 h in a conventional forced-convection drying oven. Then, an aqueous solution (50 mg/mL, 1 mL) of PVP (M_w = 630,000, Fluka) was quickly injected into the reaction solution and further heated for 6 h. The prepared NCs were

separated by centrifugation, and then washed thoroughly with water and ethanol.

FESEM images of the sample were taken with a field-emission scanning electron microscope (Phillips Model XL30 S FEG). TEM images were obtained with a Tecnai G2 F30 transmission electron microscope operating at 300 kV after placing a drop of NC solution on a carbon-coated Cu grid (200 mesh). XRD patterns were obtained with a Bruker AXS D8 DISCOVER diffractometer using Cu K_α (0.1542 nm) radiation. Raman spectra were obtained using a Jobin Yvon/HORIBA LabRAM spectrometer equipped with an integral microscope (Olympus BX 41). The 632.8 nm line of an air-cooled He/Ne laser was used as an excitation source. Raman scattering was detected with 180º geometry using an air-cooled 1024 × 256 pixel charged coupled device (CCD) detector. The Raman band of a silicon wafer at 520 cm^{-1} was used to calibrate the spectrometer. SERS sample was prepared by dropping 30 μL of a 0.1 mM ethanol solution of 4-ABT or BT onto the drop-casting film of NCs on a Si substrate. After 1 h, it was washed with ethanol and dried under ambient condition.

Acknowledgments. This work was supported by Basic Science Research Programs (2010-0029149) and PRC Program (2012-009541) through the NRF funded by the Korea government (MSIP).

References

1. Kim, F.; Connor, S.; Song, H.; Kuykendall, T.; Yang, P. *Angew. Chem. Int. Ed.* **2004**, *43*, 3673.
2. Kim, D.-S.; Heo, J.; Ahn, S.-H.; Han, S. W.; Yun, W. S.; Kim, Z. H. *Nano Lett.* **2009**, *9*, 3619.
3. (a) Heo, J.; Kim, D.-S.; Kim, Z. H.; Lee, Y. W.; Kim, D.; Kim, M.; Kwon, K.; Park, H. J.; Yun, W. S.; Han, S. W. *Chem. Commun.* **2008**, 6120. (b) Kim, D.; Heo, J.; Kim, M.; Lee, Y. W.; Han, S. W. *Chem. Phys. Lett.* **2009**, *468*, 245.
4. (a) Kown, K.; Lee, K. Y.; Lee, Y. W.; Kim, M.; Heo, J.; Ahn, S. J.; Han, S. W. *J. Phys. Chem. C* **2007**, *111*, 1161. (b) Kown, K.; Lee, K. Y.; Kim, M.; Lee, Y. W.; Heo, J.; Ahn, S. J.; Han, S. W. *Chem. Phys. Lett*. **2006**, *432*, 209. (c) Lee, K. Y.; Lee, Y. W.; Lee, J.-H.; Han, S. W. *Colloid Surface A* **2010**, *372*, 146.
5. Seo, D.; Park, J. C.; Song, H. *J. Am. Chem. Soc.* **2006**, *128*, 14863.
6. Chen, Y.; Gu, X.; Nie, C.-G.; Jiang, Z.-Y.; Xie, Z.-X.; Lin, C.-J. *Chem. Commum.* **2005**, 4181.
7. Vigderman, L.; Khanal, B. P.; Zubarev, E. R. *Adv. Mater.* **2012**, *24*, 4811.
8. (a) Lee, K. Y.; Kim, M.; Lee, Y. W.; Choi, M. Y.; Han, S. W. *Bull. Korean Chem. Soc.* **2007**, *28*, 2514. (b) Heo, J.; Lee, Y. W.; Kim, M.; Yun, W. S.; Han, S. W. *Chem. Commun.* **2009**, 1981.
9. Jeong, G. H.; Kim, M.; Lee, Y. W.; Choi, W.; Oh, W. T.; Park, Q.; Han, S. W. *J. Am. Chem. Soc.* **2009**, *131*, 1672.
10. Kim, D. Y.; Im, S. H.; Park. O. O. *Cryst. Growth Des.* **2010**, *10*, 3321.
11. Hong, J. W.; Lee, S.-U.; Lee, Y. W.; Han, S. W. *J. Am. Chem. Soc.* **2012**, *134*, 4565.
12. Phillips, F. C. *An Introduction to Crystallography*; John Wiley & Sons: New York, 1972.
13. (a) Baranrd, A. S.; Russo, S. P. *J. Phys. Chem. C* **2009**, *113*, 5376. (b) Ohashi, W.; Spaepen, F. *Nature* **1987**, *330*, 555.
14. (a) Wang, Z. L. *J. Phys. Chem. B* **2000**, *104*, 1153. (b) Wang, Z. L.; Gao, R. P.; Nikoobakht, B.; El-Sayed, M. A. *J. Phys. Chem. B* **2000**, *104*, 5417.
15. Jeong, G. H.; Lee, Y. W.; Kim, M; Han, S. W. *J. Colloid Interf. Sci.* **2009**, *329*, 97.
16. Wang, H.; Halas, N. J. *Adv. Mater*. **2008**, *20*, 82.